

Supporting information

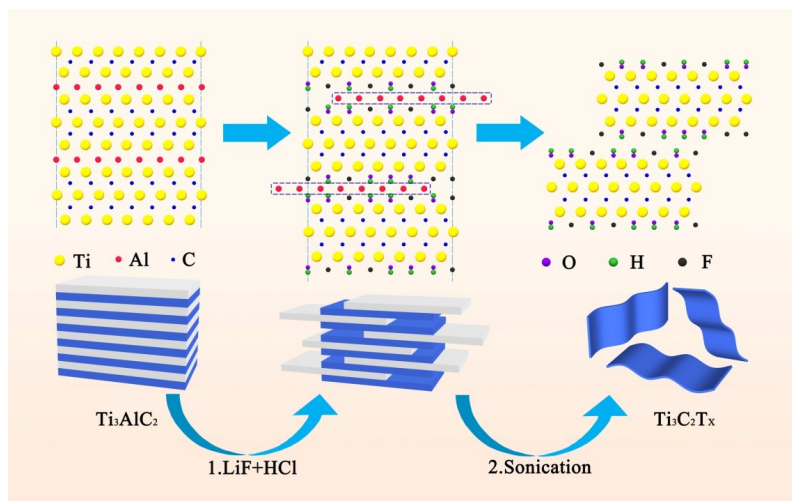
Solution-processable $\text{Ti}_3\text{C}_2\text{T}_x$ nanosheets as an efficient hole transport layer for high-performance and stable polymer solar cells

Chunli Hou^a, Huangzhong Yu^{a,b,c*}, Chengwen Huang^a

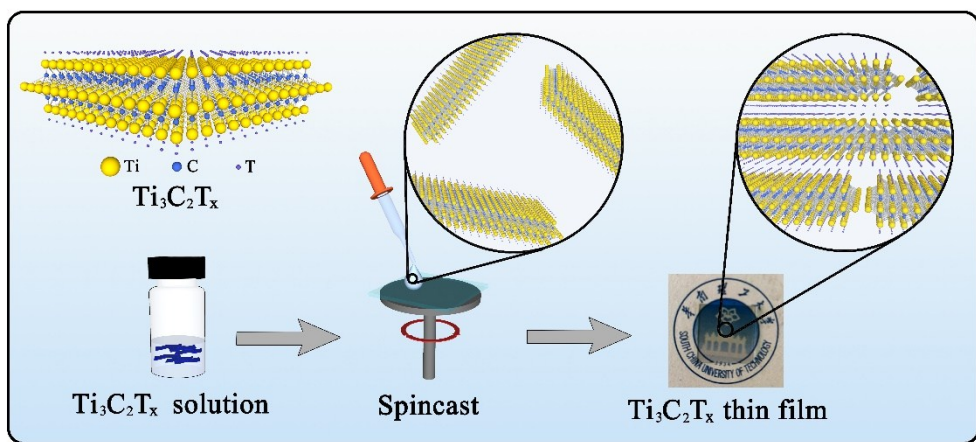
^aSchool of Physics and Optoelectronics, South China University of Technology, 510640
Guangzhou, China

^bSouth China Institute of Collaborative Innovation, 523808 Dongguan, China

^cGuangdong Provincial Key Laboratory of New and Renewable Energy Research and
Development, 510640 Guangzhou, China
Corresponding author: hzhyu@scut.edu.cn (H.Z. Yu)



Scheme S1 Schematic illustration for the synthesis of Ti₃C₂T_x.



Scheme S2 Schematic illustration for the preparation of Ti₃C₂T_x spin-casting film.

Table S1 Photovoltaic parameters of PSCs with different PEDOT:PSS thicknesses. All parameters are averaged from 10 devices.

PEDOT:PSS thickness (nm)	V_{oc} (V)	J_{sc} (mA cm ⁻²)	FF (%)	PCE (%)
46	0.90	16.15	68.37	9.94 ± 0.11
41	0.90	16.12	68.82	9.98 ± 0.11
37	0.90	16.13	69.57	10.10 ± 0.11
34	0.90	16.10	68.24	9.89 ± 0.11
29	0.90	16.06	67.93	9.82 ± 0.11
25	0.89	15.98	67.34	9.82 ± 0.11



Fig. S1 The Tyndall scattering effect in $\text{Ti}_3\text{C}_2\text{T}_x$ solution.

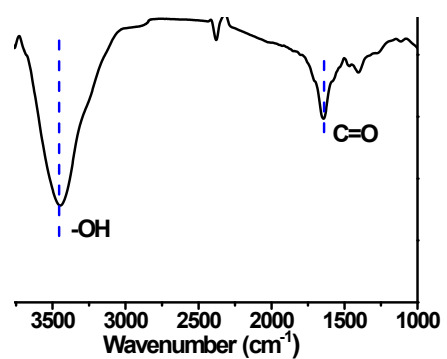


Fig. S2 FTIR spectrum of $\text{Ti}_3\text{C}_2\text{T}_x$.

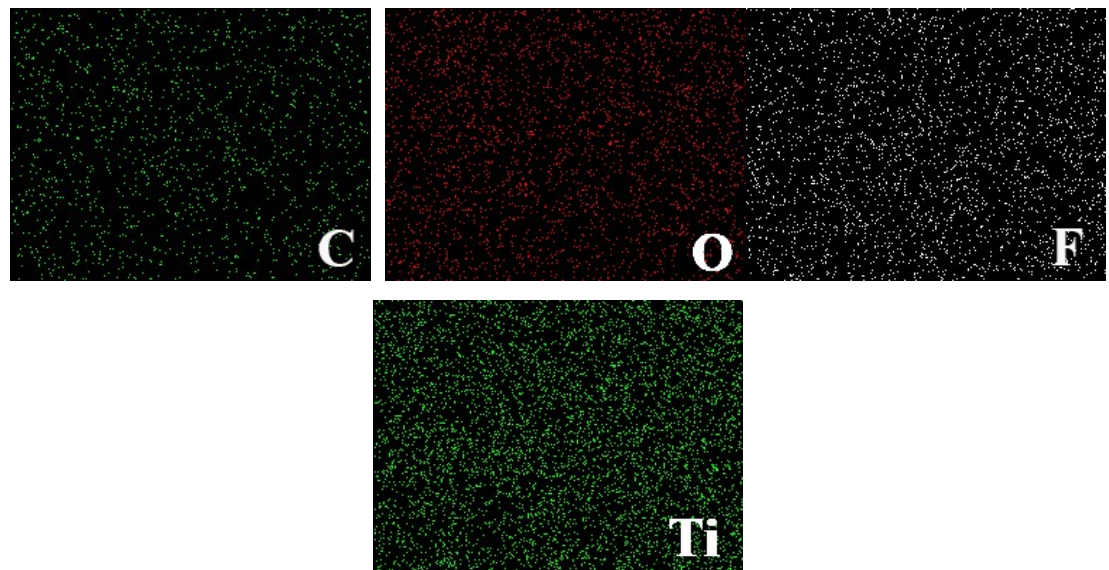


Fig. S3 Elemental maps of $\text{Ti}_3\text{C}_2\text{T}_x$.

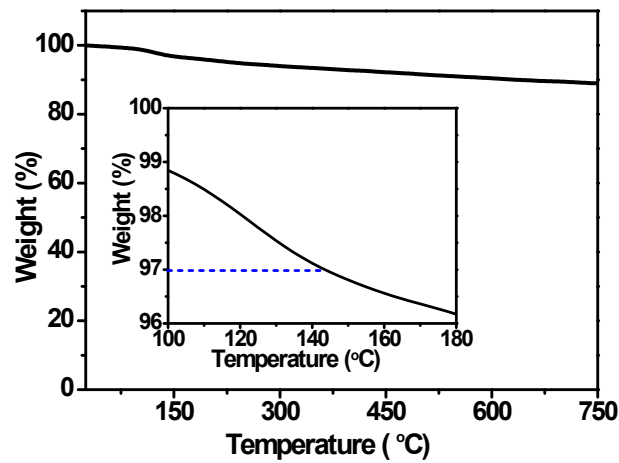


Fig. S4 TGA curve of $\text{Ti}_3\text{C}_2\text{T}_x$.

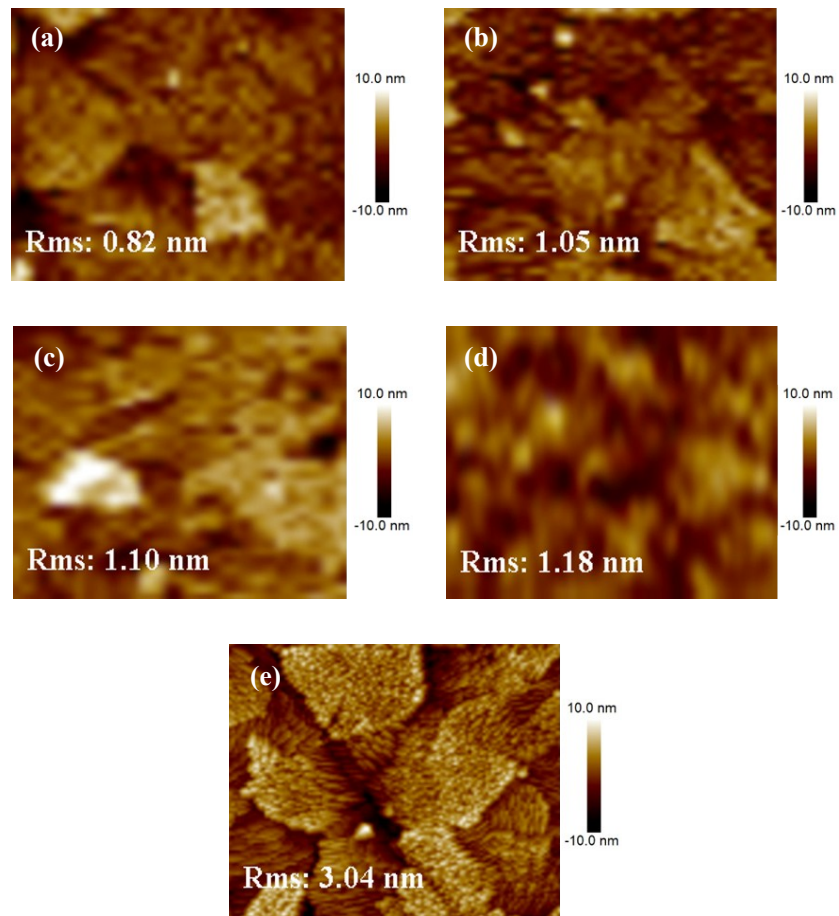


Fig. S5 AFM images of (a) $\text{Ti}_3\text{C}_2\text{T}_\text{X}$ (1.5 nm), (b) $\text{Ti}_3\text{C}_2\text{T}_\text{X}$ (3 nm), (c) $\text{Ti}_3\text{C}_2\text{T}_\text{X}$ (6 nm), (d) $\text{Ti}_3\text{C}_2\text{T}_\text{X}$ (15 nm), and (e) ITO only. All the images are $1 \mu\text{m} \times 1 \mu\text{m}$.

Table S2 The conductivities of the PEDOT:PSS and $\text{Ti}_3\text{C}_2\text{T}_x$ films on bare glass.

Device Configuration	Conductivity (S cm^{-1})
Glass/PEDOT:PSS	0.0068
Glass/ $\text{Ti}_3\text{C}_2\text{T}_x$	4035.61

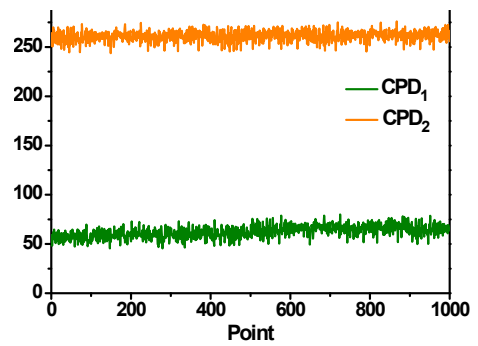


Fig. S6 CPD image of Au (CPD₁) sample and Ti₃C₂T_x (CPD₂) related to the Au reference probe.

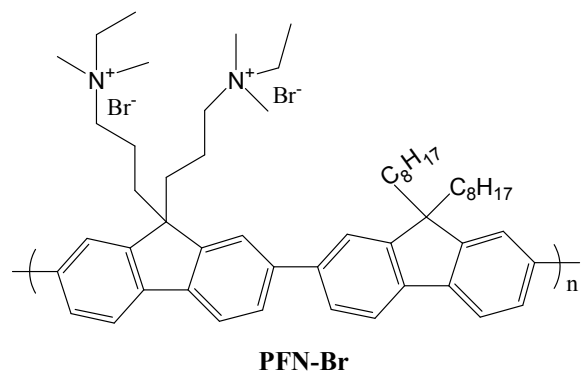


Fig. S7 Chemical structure of PFN-Br.

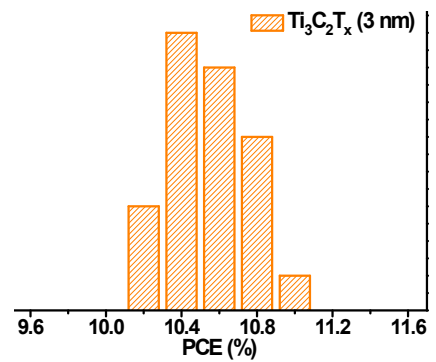


Fig. S8 Histogram of PCE counts for 24 devices based on $\text{Ti}_3\text{C}_2\text{T}_x$ (3 nm).